Low-Cost CMOS Active Array Solution for Highly Dense X-Band Weather Radar Network

Javier A. Ortiz, *Student Member, IEEE*, Jorge L. Salazar-Cerreno, *Senior Member, IEEE*, José D. Díaz, *Student Member, IEEE*, Rodrigo M. Lebrón, *Student Member, IEEE*, Nafati A. Aboserwal, *Member, IEEE*, and Laurence Jeon

***Abstract*—This article presents the development of a CMOS active array antenna unit cell as a potential solution for a highly dense, low-altitude short-coverage phased array X-band radar network system. The antenna uses a cross-patch differential feed structure designed in a stacked configuration for bandwidth and cross-polarization enhancement. To overcome the limitations of current CMOS RF performance, a mirroring technique was applied at the element and subarray level. A 16-element array (4 × 4 elements), integrated with CMOS T/R modules in a tileable architecture, was developed and characterized. Measured results demonstrate that this proposed array offers cross-polarization levels less than −32 dB across the scanning range of ±45° in the principal planes for dual-polarized alternate transmit and alternate receive (ATAR) phased array weather radar.**

***Index Terms*—Active phased array antenna, balanced feeding, dual-polarized, dual-polarized weather radar, low-profile phased array, microstrip antenna array, mirrored feed network, near field calibration, probe-fed, T/R modules.**

I. Introduction

During the last decade, interest in using rapid scanning radars for weather observation has significantly increased among meteorologists and radar engineers. Faster update radars (less than 1 min) are desirable for monitoring large-scale, fast-moving storm events, especially for the study of tornado evolutions [1]. With such agile capabilities, a single radar platform using phased array radars (PARs) offers multi-beam features that can be applied to many applications, such as air traffic control and weather observation. PARs are also scalable, reconfigurable, more reliable, and offer potential solutions for reducing the operation and maintenance costs of radar systems [1], [2].

One of the limitations of current weather radar network systems is blockage due to Earth's curvature, which obstructs observations at low levels of the atmosphere, except at distances close to the radar. A transformative concept proposed by McLaughlin and Chandrasekar [2] and McLaughlin *et al.* [3] at the CASA NSF Engineering Research Center overcomes this coverage limitation. The approach consists of the implementation of a dense radar network (about 10 000 radars) of short-range (< 40 km range), low-power (< 100 W), low-weight (< 200 lb), and low-cost (< \$100 000 per PAR) X-band PARs. CASA PARs require an aperture of 1 m × 1 m to obtain a beamwidth of 2° × 2°. A peak transmit power of 70–100 W is required in order to obtain radar coverage between 25 and 40 km. CASA PARs contain 4096 elements distributed in a rectangular lattice of half-wavelength spacing. Each element requires about 17–24 mW peak power per channel. Current RF technology in monolithic microwave integrated circuit (MMIC) devices offers a large variety of components that can satisfy the power requirement needed by this proposed array. A potential cost-effective solution is the use of integrated circuits (ICs) in CMOS or SiGe to enable a significant reduction of cost in mass production. To this day, commercial CMOS technology of 0.13 μm can deliver a transmit peak power of 12.6–31.6 mW per channel [4].

In dual-polarized weather radars, a minimum of a 0.1 dB mismatch between H- and V-co-polar patterns and high cross-polarization isolation levels are required. For simultaneous transmit and receive (STSR), less than −40 dB of cross-polarization over the scanning range of ±45° in azimuth and ±20° in elevation is necessary [5]. However, for ATAR polarization mode, cross-polarization requirements are relaxed to −20 dB [1], [6]. To achieve such requirements, high-performance RF front-ends (antennas and T/R modules) are required. To the authors' knowledge, there has not been a report of using RF CMOS T/R modules integrated into an antenna to satisfy such polarimetric requirements for ATAR polarization mode in weather PARs. The purpose of this article is to address this concern and demonstrate that PARs using CMOS technology can fulfill the need of a cost-effective, short-range, dual-polarized X-band weather radar system.

This article discusses the integration of a high-performance radiating element with a tileable, low-profile, low-cost, highly packed CMOS IC multi-core chip (MCC), and demonstrates the scanning capabilities of the array in a large-scaled polarimetric weather radar network. Section II provides a complete description of the array unit cell architecture. In Section III,

Manuscript received October 19, 2018; revised February 25, 2019; accepted April 27, 2019. Date of publication February 3, 2020; date of current version July 7, 2020. This work was supported by RFcore. *(Corresponding author: Jorge L. Salazar-Cerreno.)*

Javier A. Ortiz, Jorge L. Salazar-Cerreno, José D. Díaz, Rodrigo M. Lebrón, and Nafati A. Aboserwal are with the Department of Electrical and Computer Engineering, The University of Oklahoma, Norman, OK 73071 USA, and also with the Advanced Radar Research Center, The University of Oklahoma, Norman, OK 73071 USA (e-mail: salazar@ou.edu).

Laurence Jeon is with RFcore Company, Ltd, C-708 Pundang Technopark Yatap SungNam 463-760, South Korea.

Color versions of one or more of the figures in this article are available online at http://ieeexplore.ieee.org.

Digital Object Identifier 10.1109/TAP.2019.2947135

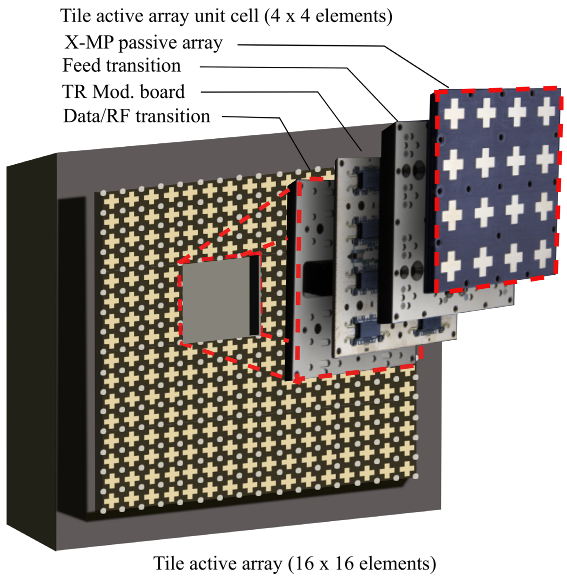

Fig. 1. Dual-polarized X-band active array antenna tile of 4×4 elements with 16 CMOS MCCs (32 channels).

the radiating element design trade-offs are discussed. The array's design and performance is demonstrated in Section IV. Section V presents the TR module technology, and Section VI discusses measured results of the array architecture.

II. Active Array Antenna Architecture

Low-profile, tileable, X-band active array antennas, T/R module technologies, and their benefits were discussed in [7] and [8]. In comparison to brick-style modules [8], [9], tileable architecture brings the ability to expand and scale the size of a PAR without compromising the mechanical design and RF performance. This architecture provides a significant reduction in space and weight that can be beneficial for space, airborne, and dense radar network applications. An active array tile architecture demands high electronic integration, and in most cases, requires customized IC designs and special electro-mechanical interfaces to interconnect the analog or digital beamformers, the heat transfer interfaces, and the front-end subassembly.

An new approach that enables a reduction in size and weight and eliminates the need for connectors, while still maintaining the RF and thermal performance of the array, consists of using a metal interface between the antenna array and the front-end T/R module board. This metal is used as a heat sink, and also provides interconnection using fuzz buttons that provide low losses and reliable RF and mechanical connection [10], [11]. This concept is illustrated in Fig. 1 where the proposed active array is used to populate a large scale array of 16×16 elements.

III. Antenna Design Trade-Offs

In this section, the proposed design and trade-offs of a balanced, probe-fed, cross-patch antenna with feed rotation at the subarray level is discussed. Emphasis is on the design

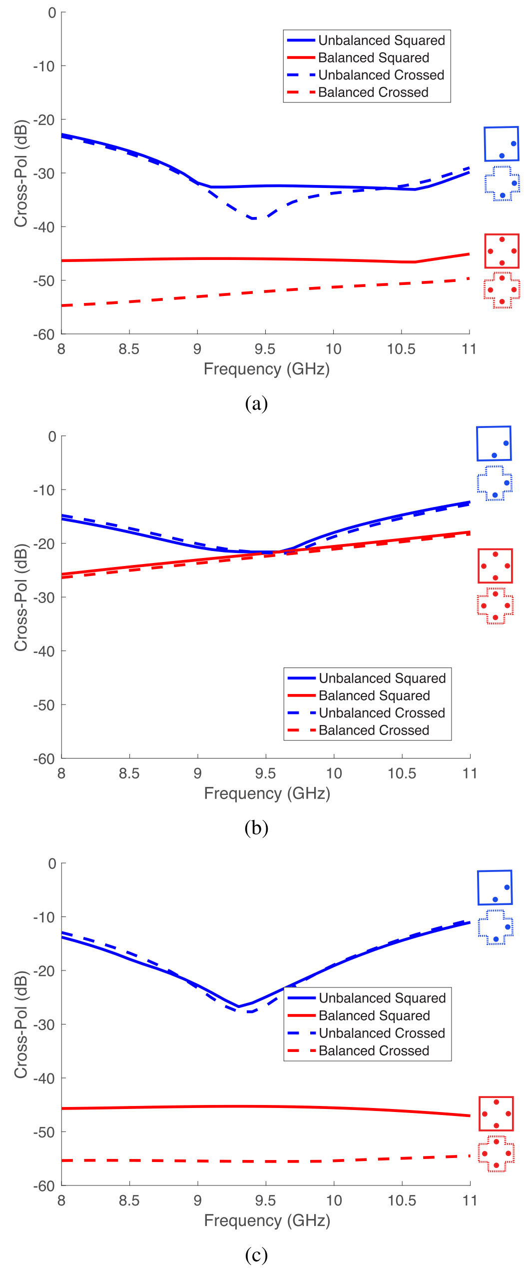

Fig. 2. Cross-polarization performance for a square and a cross-patch antenna using unbalanced- and balanced-fed techniques for (a) E-plane, (b) D-plane, and (c) H-plane.

of the radiating element and its benefits concerning isolation, cross-polarization, and scanning performance.

A square microstrip patch antenna is one of the most common radiating elements for a low-profile, dual-polarized, phased array antenna for atmospheric applications [8], [12], [13]. Square microstrip patches are highly sensitive to the accuracy of the feed position and the tight tolerances resulting from the fabrication process. It has been reported that small deviations of feed position (<5% error) induce large errors in the port isolation and cross-polarization patterns of square microstrip patches [14]. Square patch antennas also excite higher-order modes, which contaminate the cross-polarization when values are less than -30 dB.

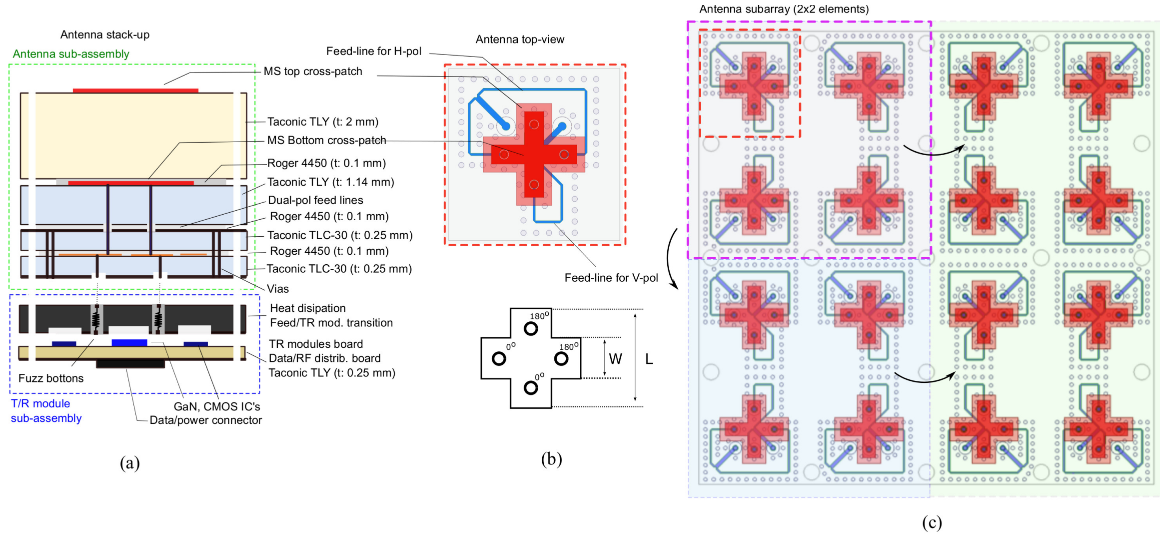

Fig. 3. Active array architecture. (a) Antenna array stack-up. (b) Antenna element geometry, where $L_p = 9.5$ mm, $W_p = 3.3$ mm, $L = 8$ mm, and $W = 1.8$ mm. (c) Antenna array geometry of 4×4 elements, indicating a subarray of 4×4 elements and a phased mirroring concept at the subarray level.

To improve cross-polarization isolation, a microstrip patch antenna was fed with a balanced network [15], [16]. A power divider that provides the same magnitude for each excited feed position with a 180° phase shift improves the cross-polarization levels to less than −30 dB. The implementation of a differential feed to balance the radiating element field excitation increases the bandwidth of the antenna [17]. Bandwidth is important for improvement in scanning performance at the array level, and also improves the axial ratio [18], [19].

To improve cross-polarization levels to less than −30 dB, printed crossed dipoles were proposed in [20]. However, these antennas are not low-profile, are sensitive to diffracted fields in the vertical structures, and are more complicated to fabricate than microstrip patch antennas when using a standard printed circuit fabrication process.

To achieve the required port isolation and array antenna cross-polarization for weather radars, a cross-patch antenna, excited with two separate and independent balance-fed networks, is proposed in this article. This approach has been successfully implemented in *L*- and *S*-band antenna elements that provided a port isolation of less than −30 dB in the principal planes [12], [21]. Also, a cross-polarization phase mirroring technique at the subarray level is recommended and also implemented for weather applications in [22]. Two-port cross-patch antennas were introduced by Vallecchi and Biffi Gentili [23] in order to design a series-fed resonant array antenna. While maintaining a symmetrical structure for dual-polarized applications, cross-patch antennas help to mitigate undesirable higher-order modes that are easily excited in a conventional square patch antenna [14]. In the design proposed in this article, a cross-patch with a four-probe balanced network is used to further improve port isolation and cross-polarization [24].

Fig. 2 presents the trade-offs between square and cross-patch antennas, with unbalanced and balanced-feeding optimized for better cross-polarization performance in the principal and diagonal (D) planes. The values shown are taken from peak cross-polarization levels in the desired scanning range (±45°). The results demonstrate how unbalanced feeding minimally affects both square and cross-patch performance with respect to cross-polarization levels. Slight improvements in isolation are seen in the E-plane [see Fig. 2(a)] of the cross-patch. A significant improvement of about 10 dB or more in cross-polarization isolation is demonstrated in the H- and E-planes [see Fig. 2(a) and (c)] when the feeding is balanced. This improvement can be attributed to a strong suppression of the higher-order modes. An additional 5–10 dB of improvement in the principal planes can be achieved by the application of a cross-patch structure as shown in Fig. 2(a) and (c). Table I presents the summary of the trade-offs for four antennas of different W/L ratios and feed techniques. In all cases the same dielectric material (TLY) (ϵ_r: 2.2 and Tanδ: 0.0009) was used. Reducing the W/L ratio increases the resonant length of the patch and relative feed position of the probe. In cases of a smaller ratio of W/L, the cross-patch antenna maintains its efficiency and impedance bandwidth.

IV. Antenna Array Design

A. Antenna Element

Fig. 3 shows the antenna element geometry and material stack-up. The antenna subassembly was composed of four dielectric layers. A layer of Taconic (TLY) (ϵ_r:2.2 and Tanδ: 0.0009), with a thickness of 2 mm, was used to separate the cross-patch and parasitic cross-patch antennas. A second layer of Taconic (TLY) with a thickness of 1.14 mm was used to separate the cross-patch and strip-line-feed networks. A strip-line-feed network was placed between the two Taconic TLC-30 (ϵ_r:3.0 and Tanδ:0.003) layers. The feeding structure was composed of two power dividers designed to apply a 180° phase shift between the ends of the strip lines. Vias were placed in the strip-line layer to mitigate parallel-plate modes in order to avoid compromising the isolation between ports. The large number of vias and probe excitations necessary for the balanced-fed network increased the inductance of the input

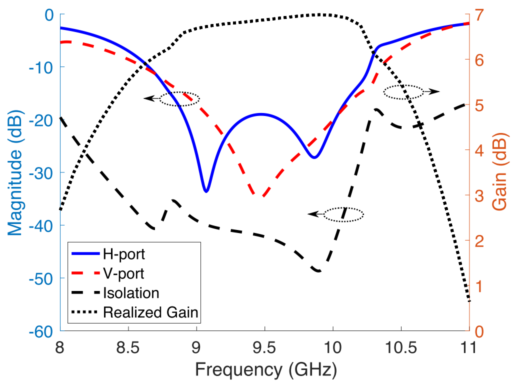

Fig. 4. Simulated S-parameters (S_{11} for H-pol, S_{22} for V-pol, and S_{21} for port isolation) and realized gain of the designed balanced-fed cross-patch antenna element.

impedance of the antenna. Capacitive gaps were introduced in the bottom radiating patch, as the annular ring slot shown in [25]. These gaps had to be carefully sized due to coupling caused by resonances in the rings that could affect the isolation of the element. Fig. 4 shows an achieved isolation of less than −40 dB across the bandwidth between the two feeding ports of the antenna element.

It has been shown that using balanced-fed microstrip patches limits scanning performance. As the beam scans, resonance anomalies appear if the feeding structure is not well isolated. In [15], scanning was improved by implementing a Wilkinson power divider for the differential feeding. Scanning performances shown in the probe-fed antennas in [26] have a range of ±35°. The proposed design overcomes this by using both ground planes and vias to isolate the elements from the feeding structure, as can be seen in Fig. 3(c).

B. Antenna Array

An active tile array of 4 × 4 elements was developed to support modular, scalable, large PAR for atmospheric research. To avoid grating lobes a square lattice array with element spacing of a half-wavelength was used in the x- and y-axes. An antenna sub-assembly of 0.1 λ_o thickness with a low dielectric constant (ϵ_r:2.2) was used to mitigate the impact of surface waves on overall scanning performance. A set of simultaneous and transcendental equations were used to estimate the propagation constant of surface waves (β_{sw}/k_o) in the antenna subassembly

$$(k_c d)^2 + (hd)^2 = (k_o d)^2(\epsilon_r - 1) \tag{1}$$

$$k_c d + \tan k_c d = hd\epsilon_r \tag{2}$$

where $h^2 = \beta^2 - k_o^2$ and d represents the substrate thickness of the antenna subassembly

$$\beta_{sw}/k_o = \sqrt{\left(\epsilon_r k_o^2 - k_c^2\right)}/k_o. \tag{3}$$

Fig. 5(a) shows the graphical solution for the surface wave propagation constant (β_{sw}/k_o) for the dominant mode (TM_0) in both polarizations. Higher-order modes for surface waves and parallel-plate modes are not excited using this antenna. For the antenna subassembly, the normalized propagation constant

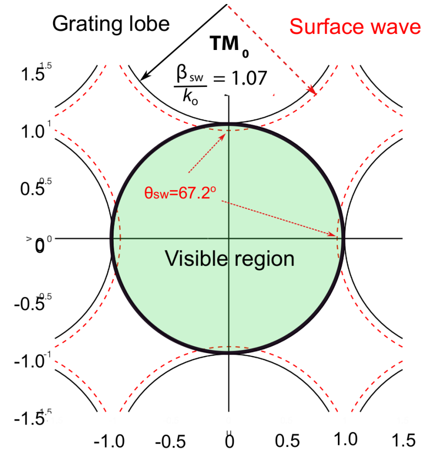

(a)

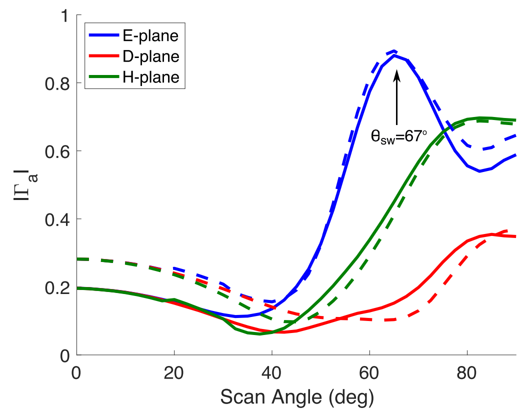

(b)

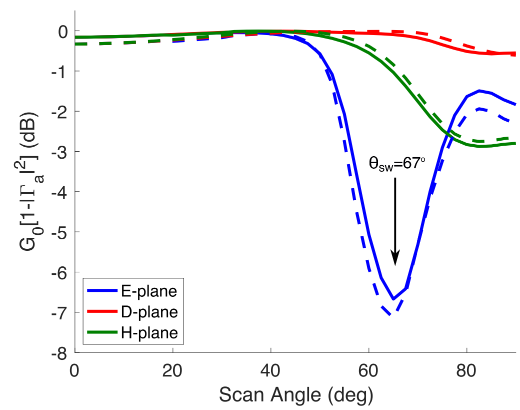

(c)

Fig. 5. (a) Grating lobe diagram showing calculated scanning performance for the proposed antenna array. (b) Simulated active reflection coefficient as a function of scan angle at 9.5 GHz. (c) Gain loss when scanning based on active reflection coefficient.

for the dominant mode (β_{sw}/k_o) is 1.07, producing a scan blindness at 67.2° for the H-pol and V-pol in the respective E-planes [see Fig. 5(b)]. Numerical simulation using an infinite array approach in HFSS validates the theoretical estimation of the scan blindness in the antenna subassembly. The scan blindness was found to be around 67° in the E-plane for both H- and V-polarizations. The active reflection coefficient (Γ_a) versus the scan angles for the E-, D-, and H-planes are represented in Fig. 5(b). Using the acquired active reflection

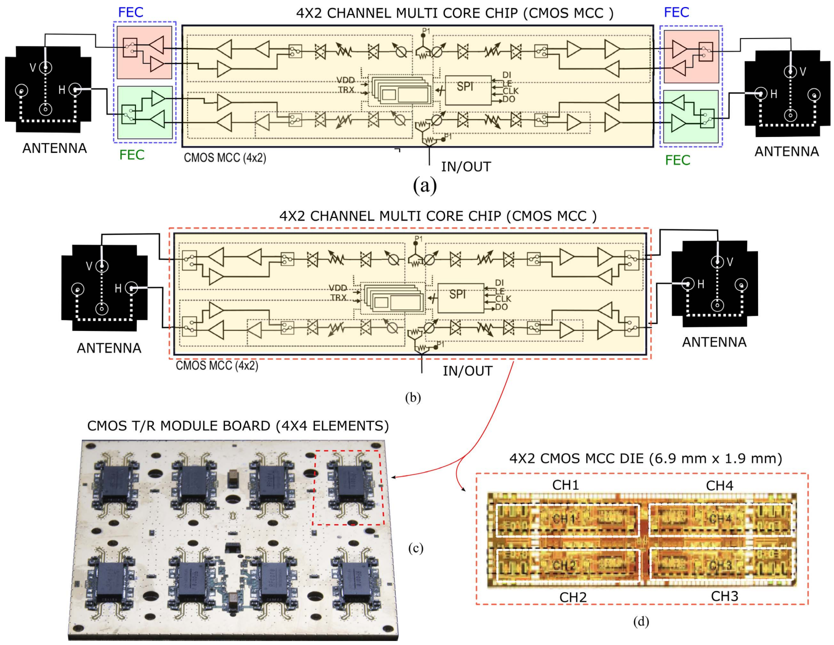

Fig. 6. (a) Block diagram of a T/R module for two elements including the 4×2 CMOS MCC and four independent GaN or GaAs FECs. (b) Block diagram of a T/R module based on a 4×2 CMOS MCC. (c) Photograph of the CMOS T/R module for the 4×4 array. (d) Representation of the four-channel CMOS MCC die.

TABLE I
ANTENNA ELEMENT PERFORMANCE TRADE-OFFS

Item/Type				
Cross ratio (W/L)	1	0.4	1	0.75
Patch length (L)	0.3 λ_o	0.39 λ_o	0.33 λ_o	0.35 λ_o
Feed position (from edge)	0.24 λ_o	0.33 λ_o	0.19 λ_o	0.21 λ_o
Cross-pol (E-plane)	-32 dB	-38 dB	-46 dB	-52 dB
Cross-pol (D-plane)	-19 dB	- 19 dB	-21 dB	-22 dB
Cross-pol (H-plane)	-27 dB	-27 dB	-45 dB	-56 dB
Bandwidth	4%	4%	21%	21%

coefficient, a calculation of a gain variation $[G_o(1 - |\Gamma_a|^2)]$ of 1 dB was obtained for the scanning range of $\pm 45°$.

In the proposed CMOS array unit cell, cross-polarization levels are limited by the attenuation performance between the antenna ports. This limitation can be easily addressed by adding a front-end chip (FEC) typically designed in GaAs or GaN. However, adding an FEC implies the use of more space that will increase the cost and complexity of the active array as illustrated in Fig. 6(a). The array architecture proposed uses a combination of CMOS MCC [see Fig. 6(b)] and a mirroring technique at the subarray level to satisfy the CASA requirements for ATAR weather radars. Mirroring techniques to reduce cross-polarization have been used before for single and dual-polarized antennas [27]–[32]. The subarray of 2×2 elements is designed as a unit cell for mirroring the feed position [see Fig. 3(c)]. Fig. 7 shows the cross-polarization phase mirroring configuration used for the array of 4×4 elements for H- and V-polarizations. This phase mirroring technique enables the cancellation of fields in order to enhance cross-polarization across the scanning range. The embedded element patterns of the subset of 2×2

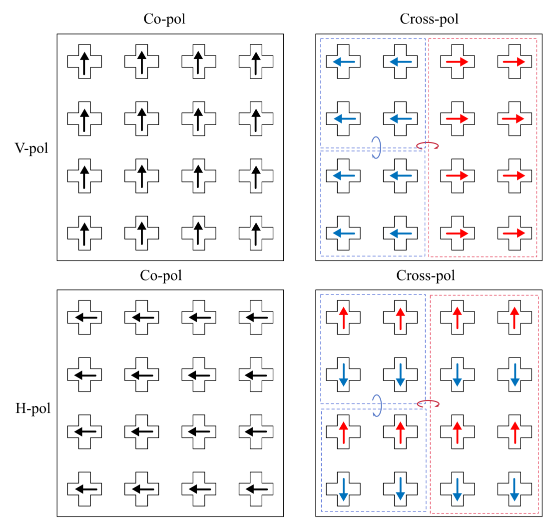

Fig. 7. Cross-polarization phase mirroring technique at the 2×2 element subarray level on a 4×4 element active array tile for H- and V-polarization.

elements of the 4×4 array are shown in Fig. 8. Due to the fact that the array is small in size, edge effects as well as mutual coupling have an impact on the cross-polarization. Furthermore, mirroring applied to H- and V-polarizations is not the same, therefore cross-polarization levels for each ports are slightly different as well.

Each channel has its independent phase shifter and attenuator capable of exciting every individual H-port and V-port at a desired phase and amplitude. As mentioned above, there is a physical mirroring inherent in the design of the antenna subarray unit cell. Therefore, there is some cancellation of fields that has to be addressed at the respective desired polarization to be transmitted. To transmit with no opposing or cancellation

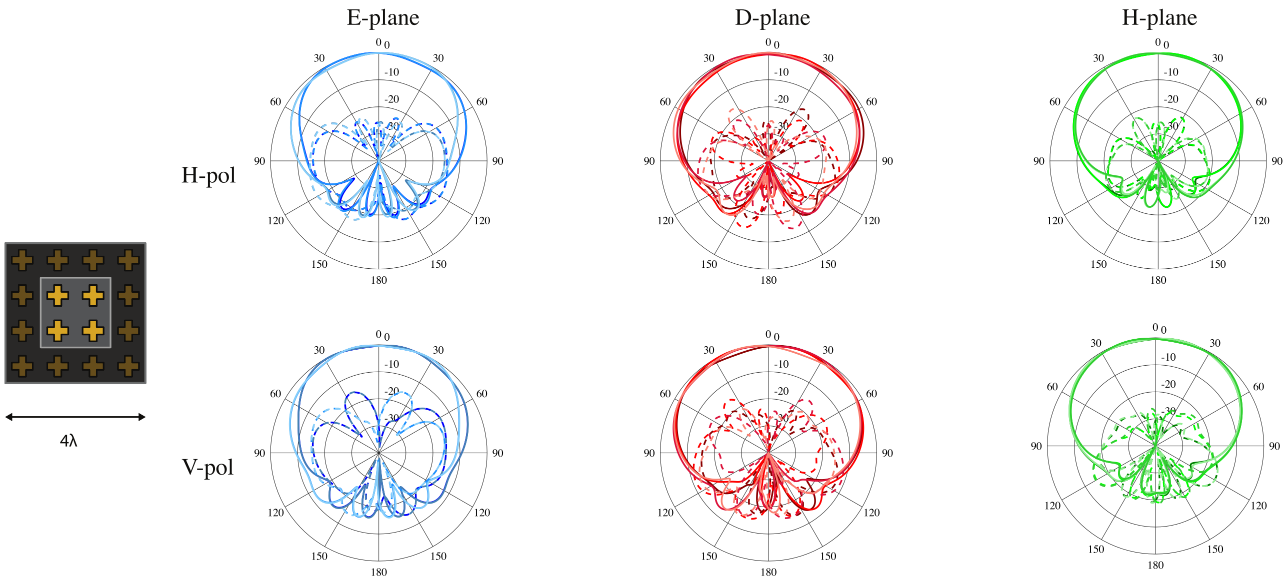

Fig. 8. Simulated (–) co- and (- -) cross-polarization embedded element patterns of the 2×2 subset in the 4×4 array unit cell at E- (in blue), D- (in red), and H-plane (in green) for V-polarization and H-polarization at 9.5 GHz.

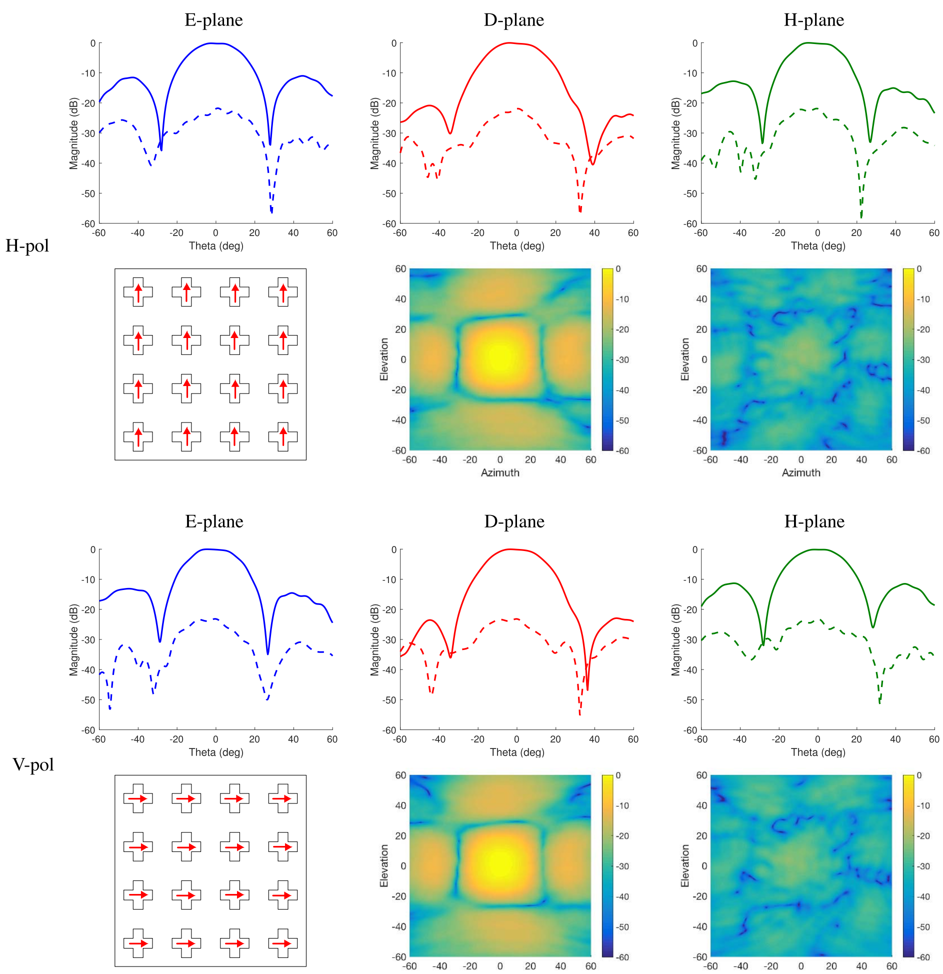

Fig. 9. Measurements of 4×4 active array patterns before applying a mirroring technique for cross-polarization components at 9.5 GHz.

of fields, as shown in the case of Fig. 9, each polarization port needs to take into account the physical mirroring for each row and column and apply a 180° phase shift so that all elements are to be added in phase. The co-pol will have no attenuation applied and the cross-pol will have minimum amplitude applied. To cancel fields for the cross-polarization

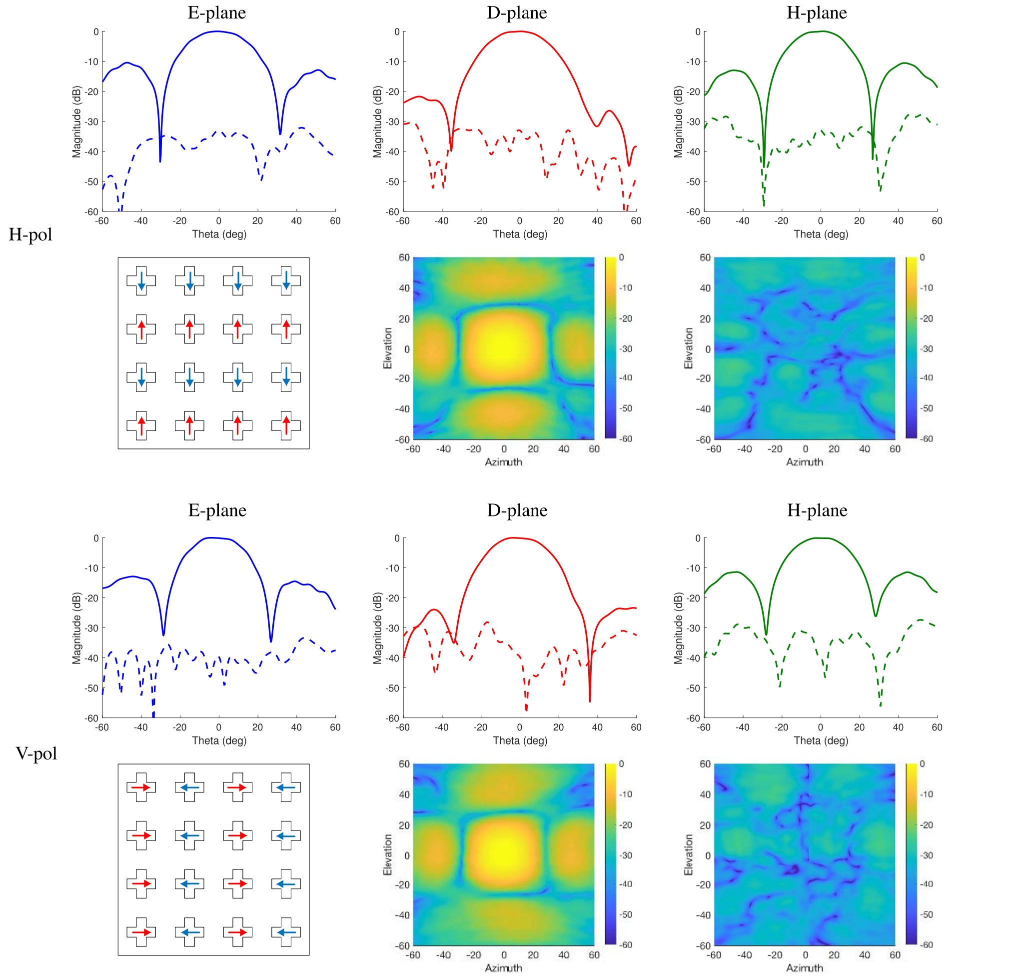

Fig. 10. Measurements of 4 × 4 active array patterns after applying a mirroring technique for cross-polarization components at 9.5 GHz.

ports, there should be no phase difference so that the physical mirroring takes place. Furthermore, if there is any other phase configuration desired to cancel cross-pol, the architecture has the ability to excite the elements at any desired phase configuration.

V. T/R Modules and Technology

For the proposed active array architecture, the T/R module design is based on an RF CMOS MCC. The MCC is a customized die developed with four channels that enable STSR and ATAR capabilities [see Fig. 6(b)–(d)]. Each channel is composed of an independent 5-bit attenuator and 6-bit phase shifter. The 0.13 μm CMOS process enables three times lower power consumption and about a 65% reduction in cost compared to GaAs core chips [8]. The MCC can transmit 11–15 dBm peak power per channel. The RMS attenuation error is 0.3 dB in amplitude and 0.9° in phase. Fig. 6(b) shows the block diagram of a T/R module board including only one MCC for two antenna elements. In the case of demand for more peak transmit power per channel in the active array, a T/R module board that includes four FECs and one MCC for two antenna elements can be implemented, as illustrated in Fig. 6(a). The FEC can be developed with GaAs or GaN on SiC to provide peak power between 1 and 10 W per channel.

TABLE II
CMOS 0.13 μM Specifications

Parameter	value
Output Tx power (dBm)	11-15
Input Rx power (dBm)	-17
Noise figure in Rx mode (dB)	7.7
RMS attenuation error (dB)	0.3
RMS phase error (°)	0.9
Channel to channel isolation (dB)	38

For a requirement of 100 W [2], each panel of 64 × 64 (4096 elements) must provide 24.4 mW of power in each element. Given the specifications of the CMOS die in Table II, each channel can reach output powers between 12.6 and 31.6 mW. Even though the implementation of the proposed FECs using GaN, as shown in Fig. 6(a), would greatly improve the performance of the architecture, the cost will be much higher. The cost for GaAs or GaN chips can be over $100 for a single channel chip in high production volume. However, CMOS can reach costs from $10 to no higher than $45 for large volumes of production [8]. The architecture presented in this article, shown in Fig. 6(b), has the advantage that

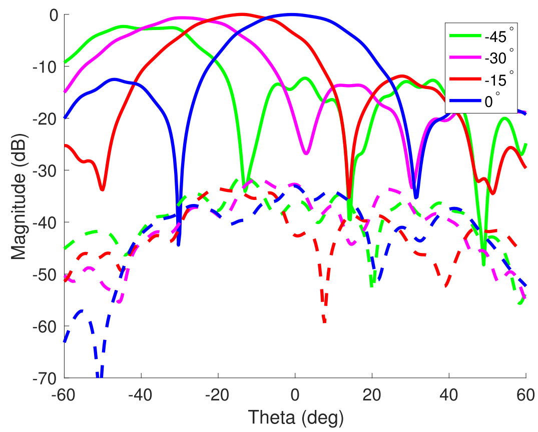

Fig. 11. Measurements of 4 × 4 active array scanned patterns in the E-plane from 0° to 45° for H-polarization at 9.5 GHz.

instead of one chip per element channel, each CMOS die has four channels, which operates two elements. For the purposes of ATAR polarization mode, CMOS technology presented in this article is enough to obtain power requirements of 100 W per panel and a large production volume cost of less than \$100 K per panel.

VI. Measured Results

A. Array Characterization and Calibration Process

To obtain a desirable amplitude and phase in each element in the array, a calibration process is needed. This process is used to account for differences in length between the electrical paths of the array channels that are caused by inherent fabrication errors of the front-end. To accomplish this, the park and probe calibration technique, mentioned previously in [33]–[35], was applied to calibrate both polarizations in each radiating element in the array. A custom made measurement system derived from [36], consisting of a six-axis robotic arm, open-ended waveguide, and a network analyzer, was used to perform the calibration in the proposed array.

B. Antenna Pattern Measurements

After calibration, the antenna patterns of the 4 × 4 array were measured. The measurements were performed using the Advanced Radar Research Center (ARRC) NF-NSI planar system. Fig. 9 shows the measured broadside antenna patterns before applying any cross-polarization phase mirroring. For both polarizations, antenna array patterns in the three planes (E-, D-, and H-planes) show cross-polarization levels around −22 dB. The shape of all cross-polar patterns is consistent with the co-polar patterns, indicating that the progressive phase is uniform. However, when applying a phase mirroring technique to the respective cross-polarized ports, which is the case presented in Fig. 10, the measured results of the antenna patterns show an improvement of about 12 dB or more for all planes. Fig. 11 illustrates the scanned patterns for the H-polarization from 0° to 45° in the E-plane, where the cross-polarization levels are maintained below −32 dB across all scan angles.

VII. Conclusion

This article presents the design and measured results of an X-band active CMOS tile subarray unit cell intended for low cross-polarization, low-profile, and low-cost phased array antennas. The proposed architecture can be used for the X-band dense radar network composed of short-range, low-power, and low-profile PARs. The use of a high-performance radiating element, integrated with highly compact RF CMOS T/R modules, was proposed for the tile subarray architecture. In order to satisfy the polarimetric requirements (cross-polarization isolation better than −20 dB across ±45° scanning range for ATAR), our team investigated a stacked cross-patch, balanced-fed antenna element with a phase-mirroring technique implemented at the subarray level. A combination of both techniques provides a viable solution to satisfy the polarimetric scanning requirements for radars in a dense network system.

A phase-mirroring technique to mitigate cross-polarization levels in the array was successfully implemented. Results show that by having the opposing polarization mirrored in each column or row of the subarray, an improvement of 12 dB or more can be achieved in all planes. Cross-polarization levels less than −32 dB were obtained across the scanning range between 0° and 45°.

Acknowledgment

The authors would like to thank J. H. Chun and S. Sim for their contributions in providing the T/R module technology. In addition, they wish to express their gratitude to M. McCord, T. Yu, and Phased Array Antenna and Development Research (PAARD) Team for supporting this project.

References

[1] D. S. Zrnic *et al.*, "Agile-beam phased array radar for weather observations," *Bull. Amer. Meteorol. Soc.*, vol. 88, no. 11, pp. 1753–1766, 2007.

[2] D. J. McLaughlin and V. Chandrasekar, "Short wavelength technology and the potential for distributed networks of small radar systems," in *Proc. IEEE Radar Conf.*, May 2009, pp. 1–3.

[3] D. Mclaughlin, E. Knapp, Y. Wang, and V. Chandrasekar, "Distributed weather radar using X-band active arrays," *IEEE Aerosp. Electron. Syst. Mag.*, vol. 24, no. 7, pp. 21–26, Jul. 2009.

[4] S. Sim, B. Kang, J. G. Kim, J. H. Chun, B. Jang, and L. Jeon, "A four-channel bi-directional CMOS core chip for X-band phased array T/R modules," in *Proc. IEEE Nat. Radar Conf.*, Jun. 2015, pp. 1198–1201.

[5] J. D. Diaz *et al.*, "A cross-stacked radiating antenna with enhanced scanning performance for digital beamforming multifunction phased-array radars," *IEEE Trans. Antennas Propag.*, vol. 66, no. 10, pp. 5258–5267, Oct. 2018.

[6] Y. Wang and V. Chandrasekar, "Polarization isolation requirements for linear dual-polarization weather Radar in simultaneous transmission mode of operation," *IEEE Trans. Geosci. Remote Sens.*, vol. 44, no. 8, pp. 2019–2028, Aug. 2006.

[7] P. Schuh *et al.*, "T/R-module technologies today and possible evolutions," in *Proc. Int. Radar Conf. Surveill. Safer World (RADAR)*, Oct. 2009, pp. 1–5.

[8] J. L. Salazar, R. H. Medina, and E. Loew, "T/R modules for active phased array radars," in *Proc. IEEE Radar Conf. (RadarCon)*, May 2015, vol. 3, no. 1, pp. 1125–1133.

[9] R. H. Medina, E. J. Knapp, J. L. Salazar, and D. J. Mclaughlin, "T/R module for CASA phase-tilt radar antenna array," in *Proc. 7th Eur. Microw. Integr. Circuits Conf.*, 2012, pp. 913–916.

[10] M. Hauhe and J. Wooldridge, "High density packaging of X-band active array modules," *IEEE Trans. Compon., Packag., Manuf. Technol. B*, vol. 20, no. 3, pp. 279–291, Aug. 1997.

[11] R. Sturdivant, C. Ly, J. Benson, and M. Hauhe, "Design and performance of a high density 3D microwave module," in *IEEE MTT-S Int. Microw. Symp. Dig.*, Nov. 1994, vol. 2, no. 6, pp. 501–504.
[12] C. Fulton, W. Chappell, and W. Lafayette, "A dual-polarized patch antenna for weather radar applications," in *Proc. IEEE Int. Conf. Microw., Commun., Antennas Electron. Syst. (COMCAS)*, Nov. 2011, vol. 2, no. 2, pp. 1–5.
[13] C. Fulton, J. Herd, S. Karimkashi, G. Zhang, and D. Zrnic, "Dual-polarization challenges in weather radar requirements for multifunction phased array radar," in *Proc. IEEE Int. Symp. Phased Array Syst. Technol.*, Oct. 2013, pp. 494–501.
[14] D. M. Pozar and B. Kaufman, "Design considerations for low sidelobe microstrip arrays," *IEEE Trans. Antennas Propag.*, vol. 38, no. 8, pp. 1176–1185, Aug. 1990.
[15] J. Hanfling, "Experimental results illustrating performance limitations and design tradeoffs in probe-fed microstrip-patch element phased arrays," in *Proc. Antennas Propag. Soc. Int. Symp.*, vol. 24, 1986, pp. 11–14.
[16] T. Chiba, Y. Suzuki, and N. Miyano, "Suppression of higher modes and cross polarized component for microstrip antennas," in *Proc. Antennas Propag. Soc. Int. Symp.*, vol. 20, 1982, pp. 285–288.
[17] P. S. Hall, "Probe compensation in thick microstrip patches," in *Proc. Microstrip Antennas, Anal. Design Microstrip Antennas Arrays*, 1995, p. 176.
[18] G. Knittel, "Relation of radar range resolution and signal-to-noise ratio to phased-array bandwidth," *IEEE Trans. Antennas Propag.*, vol. AP-22, no. 3, pp. 418–426, May 1974.
[19] M. P. David, "A review of bandwidth enhancement techniques for microstrip antennas," in *Proc. Microstrip Antennas, Anal. Design Microstrip Antennas Arrays*, 1995, p. 157.
[20] M. Mirmozafari, G. Zhang, S. Saeedi, and R. J. Doviak, "A dual linear polarization highly isolated crossed dipole antenna for MPAR application," *IEEE Antennas Wireless Propag. Lett.*, vol. 16, pp. 1879–1882, 2017.
[21] H. Wong, K. Lau, and K. Luk, "Design of dual-polarized L-probe patch antenna arrays with high isolation," *IEEE Trans. Antennas Propag.*, vol. 52, no. 1, pp. 45–52, Feb. 2004.
[22] S. Karimkashi *et al.*, "Dual-polarization frequency scanning microstrip array antenna with low cross-polarization for weather measurements," *IEEE Trans. Antennas Propag.*, vol. 61, no. 11, pp. 5444–5452, Nov. 2013.
[23] A. Vallecchi and G. Gentili, "Design of dual-polarized series-fed microstrip arrays with low losses and high polarization purity," *IEEE Trans. Antennas Propag.*, vol. 53, no. 5, pp. 1791–1798, May 2005.
[24] J. A. Ortiz *et al.*, "Ultra-compact universal polarization X-band unit cell for high-performance active phased array radar," in *Proc. IEEE Int. Symp. Phased Array Syst. Technol.*, Oct. 2016, pp. 10–14.
[25] K. Carver and J. Mink, "Microstrip antenna technology," *IEEE Trans. Antennas Propag.*, vol. AP-29, no. 1, pp. 2–24, Jan. 1981.
[26] R. B. Waterhouse, "Improving the scan performance of probe-fed microstrip patch arrays on high dielectric constant substrates," *IEEE Trans. Antennas Propag.*, vol. 43, no. 7, pp. 705–712, Jul. 1995.
[27] K. Woelders and J. Granholm, "Cross-polarization and sidelobe suppression in dual linear polarization antenna arrays," *IEEE Trans. Antennas Propag.*, vol. 45, no. 12, pp. 1727–1740, Dec. 1997.
[28] D. Vollbracht, "Understanding and optimizing microstrip patch antenna cross polarization radiation on element level for demanding phased array antennas in weather radar applications," *Adv. Radio Sci.*, vol. 13, pp. 251–268, Nov. 2015.
[29] D. Vollbracht, "Optimum phase excitations and probe-feed positions inside antenna arrays for the reduction of cross polarization radiation in demanding phased array weather radar applications," in *Proc. 10th Eur. Conf. Antennas Propag. (EuCAP)*, 2016, pp. 1–5.
[30] H. Guan-Long, Z. Shi-Gang, C. Tan-Huat, and Y. Tat-Soon, "A Ku-band 8×8 dual-polarized high-gain array with mirror-symmetric hybrid feeding network," in *Proc. 8th Eur. Conf. Antennas Propag. (EuCAP)*, 2014, pp. 653–656.
[31] S. Bhardwaj and Y. Rahmat-Samii, "Revisiting the generation of cross-polarization in rectangular patch antennas: A near-field approach," *IEEE Antennas Propag. Mag.*, vol. 56, no. 1, pp. 14–38, Feb. 2014.
[32] H. Saeidi-Manesh and G. Zhang, "Dual-linear polarization phased array antenna cross-polarization suppression using a novel image configuration," in *Proc. IEEE Int. Symp. Antennas Propag. (APSURSI)*, Jun. 2016, pp. 525–526.
[33] I. Seker, "Calibration methods for phased array radars," *Proc. SPIE*, vol. 8714, May 2013, Art. no. 87140W.
[34] J. K. Mulcahey and M. G. Sarcione, "Calibration and diagnostics of the THAAD solid state phased array in a planar nearfield facility," in *Proc. IEEE Int. Symp. Phased Array Syst. Technol.*, Oct. 1996, pp. 322–326.
[35] K. Hassett, "Phased array antenna calibration measurement techniques and methods," in *Proc. Eur. Conf. Antennas Propag. (EuCAP)*, 2016, pp. 1–4.
[36] R. Lebron, J. Salazar, C. Fulton, D. Schmidt, and R. Palmer, "A novel near-field scanner for millimiter-wave of active phased array antenna calibration for surface, thermal, and RF characterization," in *Proc. 5th Int. Symposiym Phased Array Syst. Technol.*, 2016, pp. 1–6.

Javier A. Ortiz (Student Member, IEEE) received the B.Sc. degree in electrical engineering from the University of Puerto Rico, Mayagüez (UPRM), Mayagüez, Puerto Rico, in 2013. He is currently pursuing the Ph.D. degree with the Advanced Radar Research Center (ARRC), The University of Oklahoma (OU), Norman, OK, USA.

In 2012, he co-founded the IEEE MTTS/GRS/APS Joint Chapter and was the President from 2012 to 2014. From 2013 to 2014, he was a Volunteer Laboratory Teaching Assistant and a Graduate Research Assistant at the university's Puerto Rico Weather Radar Network. He is also a Graduate Research Assistant with ARRC, OU, where he served as the Chair for the IEEE MTT-S Student Branch Chapter from 2018 to 2019. During his degree, he spent a summer at the NASA's Jet Propulsion Laboratory, Pasadena, CA, USA, where he continued the development of a hybrid simulator, which incorporates the finite-element method and physical optics for a phased array fed reflector antenna. His main research interests involve microstrip patch antennas, high-purity radiating element designs, high-performance active phased array antennas, and modeling edge effects on phased array performance using diffraction theory.

Jorge L. Salazar-Cerreno (Senior Member, IEEE) received the B.S. degree in ECE from University Antenor Orrego, Trujillo, Peru, the M.S. degree in ECE from the University of Puerto Rico, Mayagüez (UPRM), Mayagüez, Puerto Rico, and the Ph.D. degree in ECE from the University of Massachusetts at Amherst, Amherst, MA, USA. His Ph.D. research focused on the development of low-cost dual-polarized active phased array antennas (APAAs).

At NCAR, he was with the Earth Observing Laboratory (EOL) Division, developing airborne technology for 2-D, electronically scanned, dual-pol phased array radars for atmospheric research. In July 2014, he joined the Advanced Radar Research Center (ARRC), The University of Oklahoma, as a Research Scientist, and became an Assistant Professor with the School of Electrical and Computer Engineering in August 2015. His research interests include high-performance, broadband antennas for dual-polarized phased array radar applications; array antenna architecture for reconfigurable radar systems; APAA; Tx/Rx modules; radome EM modeling; and millimeter-wave antennas for automobile and communication systems.

Dr. Salazar-Cerreno was a recipient of the prestigious National Center for Atmospheric Research (NCAR) Advanced Study Program (ASP) Post-Doctoral Fellowship. In 2019, he was awarded the prestigious William H. Barkow Presidential Professorship from The University of Oklahoma.

José D. Díaz (Student Member, IEEE) received the B.Sc. degree in electrical engineering and a Curriculum Sequence in atmospheric sciences and meteorology from the University of Puerto Rico at Mayagüez, Mayagüez, Puerto Rico, in 2015. He is currently pursuing the Ph.D. degree in electrical engineering with The University of Oklahoma (OU), Norman, OK, USA, where he is involved in high-performance antenna elements for phased-array radars.

He became a Research Assistant with the Advanced Radar Research Center, The University of Oklahoma, in 2015, under the supervision of Dr. J. L. Salazar. During his studies, he spent a summer researching ultralow cross polarization antennas in Naval Research Laboratories, Washington, DC, USA. He is also a full-time Engineer with the Advanced Radar Research Center while completing his Ph.D.

Rodrigo M. Lebrón (Student Member, IEEE) was born in Asunción, Paraguay. He received the B.S. degree in mechatronics from the Universidad Nacional de Asunción, San Lorenzo, Paraguay, in 2012, and the M.S. degree in mechanical engineering from the Universidade Federal do Rio Grande do Sul, Porto Alegre, Brazil, in 2015. He is currently pursuing the Ph.D. degree in electrical and computer engineering with The University of Oklahoma (OU), Norman, OK, USA.

He was a Graduate Research Assistant with the Phased Array Antenna Research and Development Group (PAARD), hosted at the Advanced Radar Research Center (ARRC), The University of Oklahoma (OU). His research interests include design and development of automated systems for measurement, characterization, and calibration of phased-array antennas in microwave and millimeter-wave frequencies.

Nafati A. Aboserwal (Member, IEEE) received the B.S. degree in electrical engineering from Al-Mergheb University, Alkhoms, Libya, in 2002, and the M.S. and Ph.D. degrees in electrical engineering from Arizona State University, Tempe, AZ, USA, in 2012 and 2014, respectively.

In January 2015, he joined the Advanced Radar Research Center (ARRC) and the Department of Electrical and Computer Engineering, The University of Oklahoma (OU), Norman, OK, USA, as a Post-Doctoral Research Scientist. He is currently a Research Associate and a Manager of Far-Field, Near-Field, and Environmental Anechoic Chambers at the Radar Innovations Laboratory (RIL). His research interests include EM theory, computational electromagnetics, antennas, and diffraction theory, edge diffraction, and discontinuities impact on the array performance. His research also focuses on active high-performance phased array antennas for weather radars, higher modes, and surface wave characteristics of printed antennas, and high-performance dual-polarized microstrip antenna elements with low cross polarization.

Dr. Aboserwal is a member of the IEEE TRANSACTIONS ON ANTENNAS AND PROPAGATION.

Laurence Jeon received the B.S., M.S., and Ph.D. degrees from the Korea Advanced Institute of Science and Technology (KAIST), Daejeon, South Korea, in 1991, 1993, and 1998, respectively, all in electrical engineering.

He is the Founder and has been the CEO of RFcore Company, Ltd., Pundang Technopark Yatap Sung-Nam, South Korea, since November 2000. During 17 years at RFcore, he has worked with power amplifiers for mobile communication infrastructure, military radio, and IED jammers. He is now concentrating on innovative solutions for phased array RF front end. He is initiatively working for highly integrated Si/GaN chipset as well as highly integrated panel style transmitter receiver module for planar/conformal active phased array.